NONLINEAR PERFORMANCE OF MONOLITHICALLY INTEGRATED SCALN-BASED GHZ ACOUSTIC FILTERS WITH RFSOI SWITCHES

Chen Liu, Ying Zhang, Xinghua Wang, Wenjia Yang, Eugene Yi Zhun Woo, Danlei Yan, Raja M. Kumarasamy, Nan Wang and Yao Zhu

Institute of Microelectronics, A*STAR, Singapore

ABSTRACT

In this work, a comprehensive nonlinear characterization, including the 2nd order harmonic emission (H2) and the 3rd order intermodulation distortion (IMD3), has been performed on the monolithically integrated acoustic filters and RFSOI switches. The $Sc_{0.15}Al_{0.85}N$-based acoustic filters were fabricated vertically above an 8-inch RFSOI wafer. The standalone filters with different relative locations, switches and modules composing of a filter and a switch, have been characterized to evaluate the impact of the monolithic integration on the nonlinear performance of these devices. Results show that around 10 dB increase in the in-band H2 response was induced by the monolithic integration. As for the IMD3 response, the monolithic integration doesn't introduce a significant impact and the 3rd order intermodulation intercept point (IIP3) of +32 dBm can be achieved with the monolithically integrated RF module.

KEYWORDS

Monolithic integration, radio frequency, nonlinear, acoustic filter

INTRODUCTION

Scandium doped Aluminum Nitride ($Sc_xAl_{1-x}N$) is a highly attractive material for the development of advanced bulk acoustic wave (BAW) filters due to its high piezoelectric coefficient. BAW filters, providing superior performance such as high quality factor (Q), small size and great power handling capability, are dominating the high frequency (>2GHz) filtering applications in mobile phones, the Internet of Things (IoT) devices, and 5G networks. However, with the development of the wireless communication technology and the explosion of the frequency spectrum, the huge area consumption of the packaging around 100 needed acoustic filters in the mobile phone, corresponding circuitries, PCB routing and on-board impedance matching components become more and more challenging.

Monolithic integration of the acoustic filters with front-end circuitries vertically on the same wafer, instead of connecting them through on-board input-output routing, is a promising solution for addressing this integration issue [1]. Monolithically integrating the filters on CMOS wafer eliminates the need for external impedance matching components, enabling reduction of the overall device size, complexity, and package cost. Moreover, monolithic integration can improve the performance of BAW filters by reducing parasitic effects and improving device-to-device consistency.

Nonlinear behavior in BAW filters can result in signal distortion, intermodulation products, and reduced dynamic range, which can degrade the quality of the output signal and impact the ability of the filter to perform its intended function. Especially, with the expanding of the mobile spectrum to higher frequency, higher power handling performance is required by the 5G communication systems. Thus, characterizing, understanding and mitigating the nonlinear behavior of BAW filters and the composing RF modules, is crucial for developing high-performance and reliable devices [2].

Several attempts of the monolithic integration of BAW filters based on AlN on CMOS wafer have been demonstrated [3-5]. In order to implement the $Sc_xAl_{1-x}N$ to achieve a higher filter bandwidth, our group has developed a MEMS process platform to monolithically integrate $Sc_xAl_{1-x}N$-based BAW filters with single pole double throw (SPDT) switch circuit on an 8-inch RFSOI wafer. The basic radio frequency characterization has been performed and reported in IEDM 2022 [6]. In this work, the nonlinear performance of this monolithic integration, including the 2nd order harmonic emission (H2), the 3rd order intermodulation distortion (IMD3), and the 3rd order intermodulation intercept point (IIP3), have be comprehensively characterized to further examine this monolithic integration technology.

DEVICE FABRICATION

Fig. 1 (a) and (b) show the schematic and the cross-section scanning electron microscope (SEM) image of the monolithically integrated filter stack and the underneath RFSOI circuitries, respectively. An additional via process step was introduced to access the RFSOI circuits from the electrode layer of the acoustic filter stack. The SPDT switch circuit is fabricated at GlobalFoundries (GF) Singapore. The monolithic integration started with depositing SiO_2 on the top metal layer of the RFSOI wafers as passivation. The subsequent MEMS process is developed and processed using our in-house 200mm facility with all process steps with low thermal budget (< 400ºC) to avoid destruction of RFSOI circuits. The key functional stack of the BAW filter comprises 1µm-thick $Sc_{0.15}Al_{0.85}N$ film sandwiched between 150nm-thick bottom and top molybdenum (Mo) electrode layers. An additional loading layer of Al_2O_3 has been deposited on the shunt resonators in the filters to tune the resonant frequency. More details about this $Sc_xAl_{1-x}N$ MEMS process platform can be found in our previous works [6-7]. The air cavities underneath the BAW resonator and filter stack have been pre-defined and filled with sacrificial SiO_2, and finally released using vapor hydrofluoric acid (VHF) as the last step. A thin barrier layer has been implemented to protect the RFSOI circuits from corroded by VHF gas.

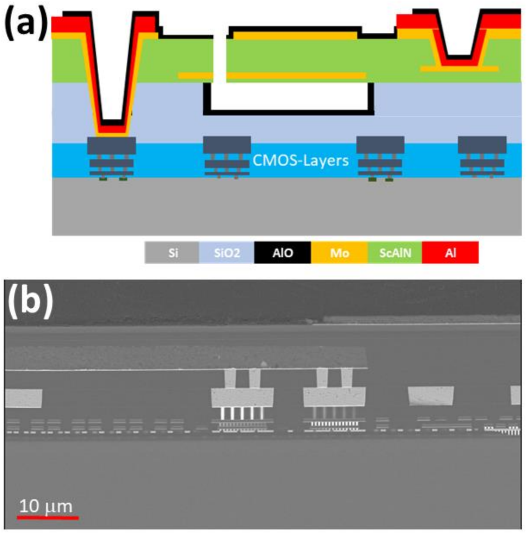

Figure 1: (a) Schematic of the cross-section of $Sc_{0.15}Al_{0.85}N$-based BAW filter on RFSOI wafer. (b) SEM cross-sectional image of the fabricated monolithic integration wafer.

NONLINEAR CHARACTERIZATION AND DISCUSSION

The setup for the characterization of nonlinear performance, including the H2 and IMD3 response, of the fabricated devices are shown in Figure 2 (a) & (b), respectively. For the H2 measurement, a train of single tones with fixed input power of 25dBm and frequency swept from 2 GHz to 2.8 GHz. To minimize the impact of high order response from the signal source, a low-pass filter was introduced between the signal source and device under test (DUT) [9]. Moreover, a duplexer is connected to the receiver end to separate the output signal from main tone and 2nd harmonic tone. For the IMD3 testing, two tones of signal (f_1, f_2) with the center frequency $f_0 = (f_1+f_2)/2$ fixed at 2.5GHz, and $\Delta f = (f_2-f_1)$ of 1MHz. As for the IIP3 testing, the input power was swept from -10 dBm to 25 dBm.

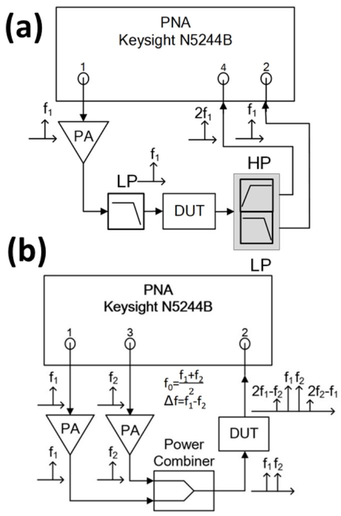

Figure 2: High power testing setup. (a) H2 testing setup; (b) IMD3 testing setup.

First, the impact of the underlying RFSOI switch on the nonlinear response of the acoustic filters was examined with different location of filters not electrically connecting to the switches, as shown in Figure 3 (a). The "above CMOS" configuration means the acoustic filters are fabricated spatial vertically above the CMOS circuits, while the "isolated" configuration means the acoustic filters are fabricated without circuits underneath. The measured output power of the fundamental tone of the standalone filters with the two layout configurations is shown in Figure 3 (b), and the 2nd harmonic output power is shown in Figure 3 (c). Results show that with close in-band output power for the fundamental tone, the "above CMOS" filter has around 10 dB larger for the H2 peak power in the filter passband, compared to the "isolated" filter. This extra 10dB H2 response difference may be introduced by the parasitic capacitors between the MEMS and RFSOI metal, and the parasitic conductors in the RFSOI layer.

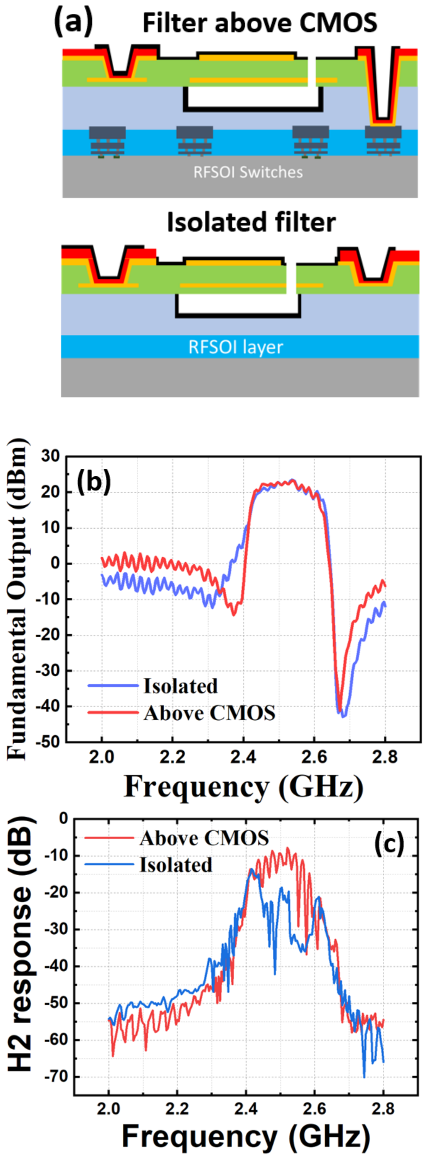

Figure 3: (a) Schematic of the filter "above CMOS" and "isolated" configurations. (b) Comparison of the fundamental output power between these two configurations. (c) Comparison of H2 response between these two configurations.

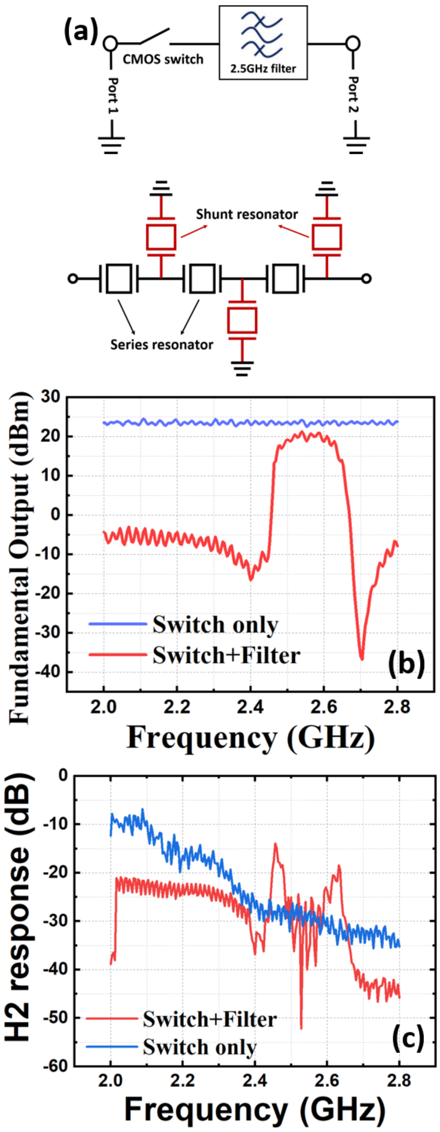

Figure 4: (a) RFSOI SPDT switch and BAW filter connection scheme. (b) Fundamental output power vs frequency for the switch and switch + filter. (c) H2 response vs input frequency for the switch and switch + filter.

Further, the nonlinear performance of the RF module composing the BAW filter and the SPDT switch was characterized. The RF path configuration in this module is the RFSOI SPDT switch connected with the BAW filter in series. And the ladder type filter in the RF module composed 3 series resonators and 3 shunt resonators. The schematic of this RF module is shown in Figure 4 (a). The measured output power of the fundamental tone of the standalone switch and the module (filter + switch) is shown in Figure 4 (b), and the 2^{nd} harmonic output power is shown in Figure 4 (c). Results show that the H2 level of the RF switch decreases with the increase of frequency, and the maximum H2 response of the module is around -15dB at the left skirt of the pass band, with input power of 25dBm injected into the module. Since in this testing the total input power is distributed in both switch and acoustic filter, the H2 response is smaller than the value in standalone filters discussed in Figure 3.

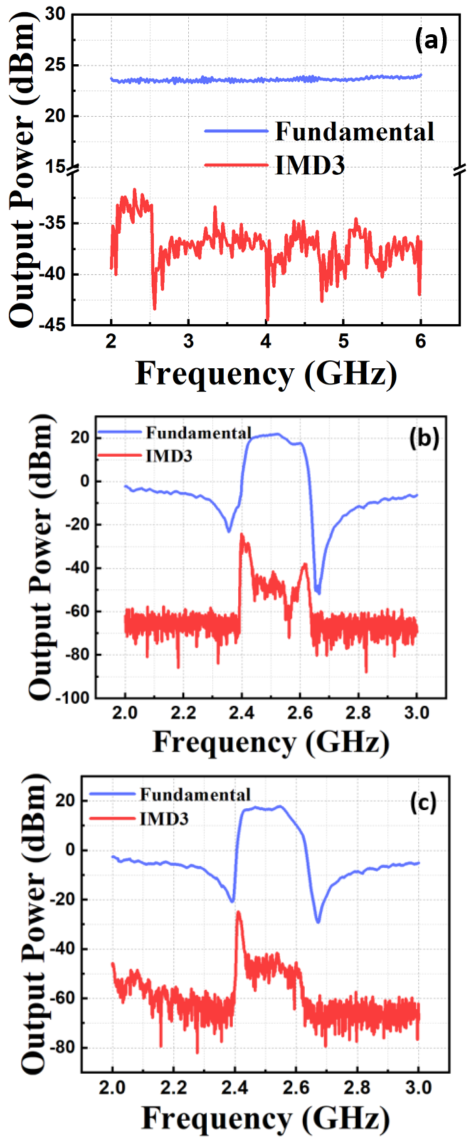

Figure 5: Fundamental and IMD3 response vs frequency of: (a) Switch alone; (b) Filter alone; (c) Switch + filter.

The fundamental and IMD3 responses vs frequency curves of the switch, standalone filter and the module (switch + filter) are shown in Figure 5 (a), (b) & (c), respectively. The IMD3 output of the standalone switch is around -35 - -40 dBm from 2 GHz to 6 GHz, and the IMD3 response of the standalone filter has a larger power level of -25 - -40 dBm inside the passband and smaller power level of -60 dBm out of the pass band. As for the RF module, a large IMD3 peak of around -25 dBm occurs at left skirt of the passband. Comparing the results of the standalone switch, filter, and the module, it indicates that this monolithic integration doesn't introduce a significant impact on the IMD3 performance of the BAW filters.

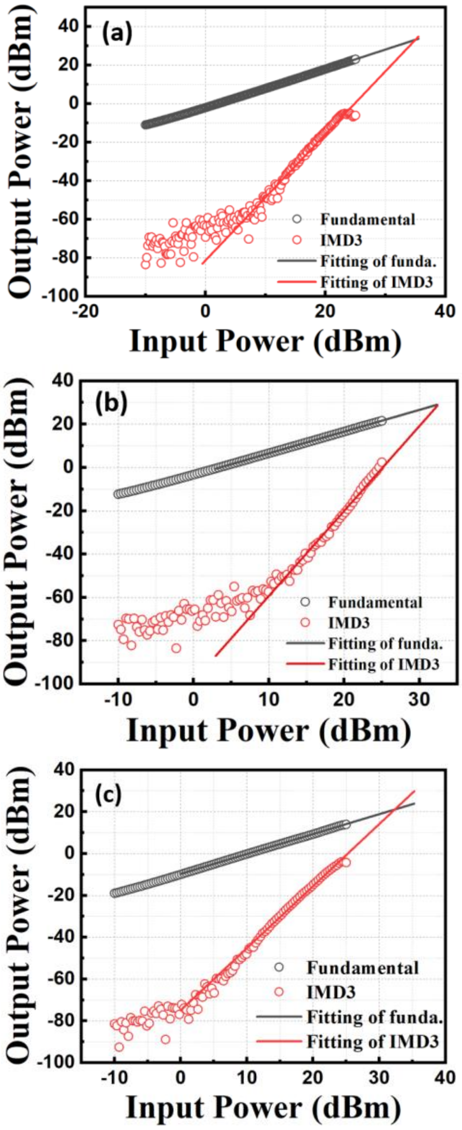

Figure 6: Two-tone power sweep characterization results of: (a) Switch alone; (b) Filter alone; (c) Switch + filter.

To check the dynamic input power of the monolithically integrated RF module, the 3rd order intermodulation intercept point of the standalone switch, filter, and the module was measured with sweeping input power swept from -10 dBm to 25 dBm, as shown in Figure 6 (a) – (c). The measured output power of the fundamental and IMD3 are linearly fitted and produced to intersect at the IIP3 point. In this way, the IIP3 of the switch, standalone filter and the module is +35.24 dBm, +32.35 dBm and +32.30 dBm, respectively. The nonlinear performances of the monolithically integrated BAW filters and the modules are yet comparable to the commercial products and the BAW filters fabricated by standalone MEMS process, thus need further improvement [8-9].

CONCLUSION

In this paper, the $Sc_{0.15}Al_{0.85}N$-based acoustic filters were fabricated vertically above an 8-inch RFSOI wafer and connected with the RFSOI switches in series. To examine the nonlinear performance of the switches, the standalone filters and the RF modules composing both filters and switches, high power testing has been performed on these devices, including the 2nd order harmonic emission (H2), the 3rd order intermodulation distortion (IMD3), and the the 3rd order intermodulation intercept point (IIP3). Measurement results on the standalone filters show that the monolithic integration process will enlarge the H2 response, probably because of parasitics introduced by the underneath CMOS. The H2, IMD3 and IIP3 results of the RF modules have been reported and results show that further improvement is needed to reduce these nonlinearity of this monolithic integration.

ACKNOWLEDGEMENTS

The authors would like to acknowledgement the strong support from Globalfoundries Singapore, especially Jason Wong, Lee Mien Sze and Peck Yan Zheng, on the test chip tapeout and RFSOI process customization.

This work was supported by the Science and Engineering Research Council of A*STAR (Agency for Science, Technology and Research) Singapore, under Grant No. A20G9b0135.

REFERENCES

[1] Uranga, J. Verd, and N. Barniol, “CMOS-MEMS resonators: From devices to applications,” Microelectronic Engineering, 132, pp. 58–73, 2015

[2] S. Fouladi et al., “FBAR Resonators Fabricated on Insulating Substrates with Improved RF and Nonlinear Performance,” IEEE Int. Ultrason. Symp. IUS, vol. 2019-Octob, pp. 88–92, 2019

[3] Dubois, M.-A., et al., "Monolithic above-IC resonator technology for integrated architectures in mobile and wireless communication", IEEE Journal of Solid-State Circuits, 2005. 41(1): p.7-16.

[4] Campanella, H., et al., "Monolithic Multiband MEMS RF Front-End Module for 5G Mobile," Journal of Microelectromechanical Systems, 2021, 30, p. 72-80.

[5] Campanella, H., et al. "Monolithic MEMS filter banks on RFSOI front-end module, " IEEE 33rd International Conference on Micro Electro Mechanical Systems (MEMS). 2020, p.218-221.

[6] Ying Zhang, et al., “3D Monolithic Integration of ScAlN-based GHz MEMS Acoustic Filters on 200mm RFSOI Wafer”, IEEE International Electron Devices Meeting (IEDM), 2022, p. 374-377

[7] N. Wang, Y. Zhu et al., “Over 10% of k2 eff Demonstrated by 2-GHz Spurious Mode-Free $Sc_{0.12}Al_{0.88}N$ Laterally Coupled Alternating Thickness Mode Resonators”, IEEE Electron Device Letters, 40, 6, 2019, p.957-p.960.

[8] H. Campanella, L. Khine, and J. M. Tsai, “Aluminum nitride lamb-wave resonators for high-power high-frequency applications,” IEEE Electron Device Lett., vol. 34, no. 2, pp. 316–318, 2013

[9] Y. Zhang et al., “Experimental and Numerical Study on the Second Order Harmonic (H2) and Third Order Intermodulation Distortion (IMD3) Response of Scandium Aluminum Nitride Based FBAR Devices with Different Scandium Doping Levels,” IEEE Int. Ultrason. Symp. IUS, pp. 5–7, 2022

CONTACT

*Chen Liu, liuc@ime.a-star.edu.sg
*Yao Zhu, zhuya@ime.a-star.edu.sg